



# Silver nanoparticles-induced nephrotoxicity in rats: the protective role of red beetroot (*Beta vulgaris*) juice

Tarfa Albrahim<sup>1</sup>

Received: 21 February 2020 / Accepted: 9 June 2020 / Published online: 7 July 2020  
© Springer-Verlag GmbH Germany, part of Springer Nature 2020

## Abstract

The present study was designed to investigate the nephrotoxicity of silver nanoparticles (AgNPs; 80 mg/kg; > 100 nm) and to evaluate the protective effect exercised by *Beta vulgaris* (beetroot) juice (RBR; 200 mg/kg) on male rats' kidney. Serum-specific parameters (urea, creatinine, electrolytes and histopathology of kidney tissue) were examined to assess the AgNPs nephrotoxicity effect. Moreover, this study analysed oxidative stress (lipid peroxidation, glutathione, superoxide dismutase and catalase) and anti-apoptotic markers (Bcl-2). AgNPs intoxication increased kidney function marker levels and lipid peroxidation and decreased the glutathione, superoxide dismutase and catalase activities in kidney tissue. Additionally, Bcl-2 expression was downregulated following AgNPs intoxication. Moreover, AgNPs induced a significant increase in renal DNA damage displayed as an elevation in tail length, tail DNA percentage and tail moment. Interestingly, RBR post-treatment restored the biochemical and histological alterations induced by AgNPs exposure, reflecting its nephroprotective effect. Collectively, the present data suggest that RBR could be used as a potential therapeutic intervention to prevent AgNPs-induced nephrotoxicity.

**Keywords** Silver nanoparticles · Red beetroot · Oxidative stress · Bcl-2 expression · Kidney toxicity

## Introduction

Silver nanoparticles (AgNPs) are present in many consumable products such as topical antibacterial formulations, hygiene sprays, food additives, baby products and kitchen utensils (Alajmi et al. 2019; Bao et al. 2020). However, to date, AgNPs full toxicity profile has not been fully clarified. It has been recommended that in vivo and in vitro nanotoxicological studies should be carried out in order to understand it (Lekamge et al. 2018; Tortella et al. 2020). Due to the small sizes of nanoparticles, they penetrate easily the membrane barriers (El-Borady et al. 2020). In this regard, AgNPs can enter the living organism easily through the dermal, inhalation and oral routes.

After that, circulation facilitates Ag accumulation in various tissues and organs such as the spleen, liver, kidney and brain. Inside the cells, Ag can induce failure and dysfunction of vital macromolecule structures such as DNA, RNA and proteins (Abramenko et al. 2018; Fukushima et al. 2020).

Some reports suggest that AgNPs toxicity is largely attributed to the release of Ag<sup>+</sup> ions upon entering the cytoplasm (El-Khadragy et al. 2018). It is still unclear which molecular and cellular mechanisms are employed by AgNPs to exert unwanted side effects at the cellular level. However, several studies have suggested that AgNPs possess the ability to induce cytotoxicity by increasing production of reactive oxygen species (ROS), inducing apoptosis, causing DNA damage and stimulating pro-inflammation. Furthermore, Li et al. (2018) reported that AgNPs tend to accumulate in the mitochondria, causing dysfunction following reduction in mitochondrial membrane potential, therefore explaining the enhanced ROS formation. Hence, there is a need to explore AgNPs toxicity-related issues in further detail by utilising appropriate experimental animal models to analyse in vivo kidney function.

Recently, the health beneficial effects of *Beta vulgaris* (*B. vulgaris*) have attracted scientific attention for its role in preventing and treating different human diseases. *B. vulgaris* is widely used worldwide, and it is known as Shamander in

Responsible editor: Mohamed M. Abdel-Daim

**Electronic supplementary material** The online version of this article (<https://doi.org/10.1007/s11356-020-09671-7>) contains supplementary material, which is available to authorized users.

✉ Tarfa Albrahim  
tialbrahim8@gmail.com

<sup>1</sup> College of Health and Rehabilitation Sciences, Department of Health Sciences, Clinical Nutrition, Princess Nourah Bint Abdulrahman University, Riyadh, Saudi Arabia

the Middle East countries. The plant belongs to the sub specie *vulgaris* of the Amaranthaceae family. The roots contain rich amounts of red- to violet-coloured pigments, including betaxanthins and betacyanin (betanin, isobetainin, probetanin and neobetainin) from the betalain family, or yellow- to orange-coloured betaxanthins (Abd El-Ghffar et al. 2019). *B. vulgaris* is highly safe, and the estimated acute lethal dose ( $LD_{50}$ ) of *B. Vulgaris* rats was found to be higher than 2000 mg/kg, which is considered relatively safe (Abd El-Ghffar et al. 2019; Jain and Singhai 2012). The roots have been used in traditional medicine to cure depression, hepatotoxicity, hypertension, hyperglycaemia and autoimmune diseases (Martinez et al. 2015; Mohammed et al. 2019; Szaefer et al. 2014).

The present study aimed to evaluate the toxic effects of AgNPs on the kidney of male rats and to examine the nephroprotective role of beetroot.

## Materials and methods

### Chemical silver nanoparticles

The chosen silver nanoparticles (AgNPs) had a diameter less than 100 nm and were purchased from Sigma-Aldrich (St. Louis, MO, USA). AgNPs were prepared by dissolving the powder in 0.5% aqueous solution of sodium carboxymethylcellulose (CMC; Sigma-Aldrich). Transmission electron microscopy (TEM), Zeta potential analyses, dynamic light scattering (DLS) and UV/Visible spectral measuring to assurance materials consistent (monodisperse AgNPs free from agglomeration; refractive index  $n_{20/D}$  1.333; fluorescence- $\lambda_{em}$  388 nm) are available at the supplier website (<http://www.sigmaaldrich.com/materials-science/nanomaterials/silver-nanoparticles.html>). Immediately prior to injection in male rats, the prepared AgNPs solution was sonicated for 10 min, according to Kim et al. (2010).

### Beetroot preparation and extraction

Fresh red beetroot was obtained from a local market located in Riyadh, KSA. Red beetroots were cleaned with tap water, sliced into small pieces, homogenised with distilled water (1:2 w/v), filtered through a filter paper and lyophilised to powder, according to the described method of Albasher et al. (2019). The prepared powder was reconstituted in distilled water to prepare red beetroot (RBR) juice at 200 mg/3.5 ml  $H_2O$ .

### HPLC analysis

HPLC (high-performance liquid chromatography) analysis was performed via a Merck-Hitachi L-7200 with Merck-Hitachi L-7400 UV/VIS detector. The HPLC column was a

C18 column (Phenomenex, Torrance, CA), and the sample was monitored by UV–Vis absorption at 280 nm. Elution was carried out using acetonitrile (A) and formic acid water (5:95, v/v) (B). The flow rate was set at 0.5 ml/min throughout the run, linear gradient from 5 to 20% B in 60 min at 25 °C and flow rate at 10 ml/min.

### Determination of total polyphenol and flavonoid content in RBR

Within the prepared RBR juice, the amount of polyphenols (PP) was estimated utilising the Folin-Ciocalteu procedure, while total flavonoid (TF) quantity was measured implementing the aluminium chloride method, based on the procedures described by Abdel Moneim (2013). Both PP and TF amounts were presented as mg gallic acid equivalent/ml juice (mg GAE/ml RBR) and mg quercetin equivalent/ml juice (mg QE/ml RBR) using gallic acid and quercetin standard calibration curves. The gallic acid calibration curve was calculated when  $Y = 0.0107X + 0.0508$  (where  $X =$  mg GAE/ml RBR and  $Y =$  optical density), and the correlation coefficient was  $R^2 = 0.9998$ , while the quercetin calibration curve was estimated according to  $Y = 0.0031X + 0.0160$  (where  $X =$  mg QE/ml RBR and  $Y =$  optical density), and the correlation coefficient was  $R^2 = 0.9997$ .

### Experimental design

Forty male Wistar albino rats (12 weeks old,  $150 \pm 20$  g weight) were maintained on standard rodent diet and tap water ad libitum. The study protocols were approved by the Ethics Committee for Laboratory Animal Care of Princess Nourah bint Abdulrahman University in Riyadh (KSA; H-01-R-059; IRB long number: 19-0201). After acclimatisation, they were divided into four groups randomly: group 1 (Con) served as control receiving normal saline solution (0.9% NaCl) and intraperitoneally injected with saline solution containing 0.5% CMC; group 2 (RBR) was administered orally with RBR juice (200 mg/kg RBR/day) and intraperitoneally injected with saline solution containing 0.5% CMC; group 3 (AgNPs) was injected intraperitoneally with AgNPs (80 mg/kg; > 100 nm) for 4 weeks and group 4 (AgNPs + RBR) was injected with AgNPs for 4 weeks (like group 3), followed by treatment with RBR for another 4 weeks at the aforementioned doses. The AgNPs dose was chosen according to previous work of Singh et al. (2018), while the RBR dose was selected according to the study of El Gamal et al. (2014).

All tested animals were euthanized with intraperitoneal injection of sodium pentobarbital (300 mg/kg i.p.) 24 h after last treatment. Blood samples were collected by cardiac puncture into non-heparinised tubes and centrifuged at  $3000 \times g$  for 15 min, to separate the serum, and stored at  $-80$  °C for kidney function marker analysis.

## Kidney function markers

The indicators for kidney damage, identified as urea, creatinine and electrolytes (potassium, sodium, calcium and chloride ions), were determined using commercial kits obtained from Randox Laboratory (Crumlin, UK) following the manufacturer protocols.

## Preparation of kidney homogenates

The right kidney from all groups were excised, weighed and homogenised in 50 mM phosphate buffer saline, pH 7.4, to prepare a 10% w/v homogenate. The homogenates were centrifuged at  $3000 \times g$  for 10 min to separate the supernatant that was then stored at  $-80^\circ\text{C}$  for further analysis.

## Oxidative stress status measurements

The kidney supernatants were used to evaluate oxidative stress markers. The analysis of lipid peroxidation (LPO) was estimated based on measuring the quantity of formed malondialdehyde (MDA), an end-product marker for lipid peroxidation, according to the method described by Ohkawa et al. (1979). The concentration of reduced glutathione (GSH) was assayed according to the protocol elucidated by Ellman (1959). The renal activity of superoxide dismutase (SOD) and catalase (CAT) was determined based on the procedures of Nishikimi et al. (1972) and Aebi (1984), respectively.

## Comet assay (determination of DNA damage)

A comet assay (single-cell gel electrophoresis) was performed to determine and quantify the levels of renal DNA damage based on the established method of Olive and Banáth (2006). Briefly, cell suspensions were embedded in 1% agarose gel on precoated slides with 0.3% agarose gel. After that, gels were dried in dark, placed in a lysis buffer and stored overnight at  $4^\circ\text{C}$  to lyse the cells and separate DNA from the histones. Subsequently, the slides were immersed in an alkaline buffer (0.3 M NaOH, 1 mM EDTA), and alkaline electrophoresis with circulating ice-cold electrophoresis buffer was performed (40 min, 17 V/cm, 0.700 A). Thereafter, slides were neutralised in 0.4 M Tris for  $2 \times 5$  min and in  $\text{H}_2\text{O}$  for 5 min. Gels were dried overnight and fixed with methanol for 5 min prior to staining of the DNA with ethidium bromide (1  $\mu\text{g}/\text{ml}$ ) in Tris-acetate-EDTA buffer. The DNA strand breaks are estimated as the % of DNA in the comet tail and as the comet tail length under a fluorescence microscope using the program Komet 4.0.

## Histological examination

The left kidney was immediately dissected, cut into small pieces and fixed in 10% neutral buffered formalin solution for 24 h. The fixed tissue was then dehydrated, cleared and embedded in paraffin wax. Sections of 5  $\mu\text{m}$  thickness were obtained using a rotary microtome (Leitz, Wetzlar, Germany) and stained with haematoxylin and eosin (Drury and Wallington 1981). For AgNPs detection in the kidney tissue, semi-thin sections were prepared on glass slides through cutting at 1  $\mu\text{m}$  using an ultramicrotome (EM UC7 from Leica Microsystems). Sections were stained with toluidine blue for 25 sec and examined with a light microscope as described by Daoust and Molnar (1964). A semi-quantitative examination of renal lesions was done by modification methods of Racusen et al. (1999). The scores of all sections were added to obtain the total score, which varied from 0 to 15. Then, a computer image analysis was applied using ImageJ software (National Institutes of Health, Bethesda, MD, USA) to quantitatively measure the glomerular capillary tuft area and glomerulus diameter.

## Anti-apoptotic (Bcl-2) protein expression

Immunohistochemistry analysis was performed to analyse Bcl-2 protein expression by incubating the kidney sections with a polyclonal anti-Bcl-2 antibody (1:200; catalogue number: sc-7382; Santa Cruz Laboratory). After three wash steps with phosphate buffered solution, sections were incubated with biotin-conjugated secondary antibody (1:500) for 1 h. Following further washes as described above, the sections were incubated with streptavidin-HRP conjugate (LSAB System HRP). The immune reaction was developed by 3'-diaminobenzidine tetrahydrochloride (DAB, DAKO Japan Co, Ltd, Tokyo, Japan) for 10 min. The sections were counterstained with haematoxylin, according to Harrison-Bernard et al. (1997).

## Statistical analysis

Results were expressed as mean values  $\pm$  standard error (SE). The data were checked for normal distribution using a parametric test, and then different assessments were evaluated statistically using one way ANOVA followed by Duncan's Multiple Range test post hoc test was used to determine significant differences among the various tested groups. A level of  $p < 0.05$  was considered to be statistically significant. All statistical analyses were performed using SPSS statistical version 21 software package (SPSS® Inc., USA).

## Results

### HPLC fingerprint of RBR juice

The polyphenol and flavonoid fingerprint of the RBR juice monitored at 280 nm is presented in Fig. 1 and Supplementary Table 1. The HPLC profile of RBR juice indicates the presence of 14 peaks. Based on the UV–Vis spectrum data and literatures, the RBR juice has a UV band at 280 nm characteristic for polyphenol and flavonoid compounds, possibly cinnamic, vanillic, chlorogenic, catechin, caffeic, coumaric, ferulic, rutin, and gallic acids and its derivatives.

### Polyphenol and flavonoid contents in RBR juice

Quantitative evaluation of PP and TF content of RBR was found to be  $18.2 \pm 1.4$  mg GAE/ml RBR and  $117.6 \pm 2.5$  mg QE/ml RBR, respectively.

### Effect of AgNPs and/or RBR juice on rats and kidney markers

Although no death was observed in any of the groups, the rats that were orally exposed to AgNPs over a period of 4 weeks appeared unhealthy, and increased breathing rate and decreased activity were observed. The severity of these signs reduced with RBR administration.

Data shown in Table 1 demonstrated that AgNPs-treated rats exhibited a significant increase in serum urea and creatinine levels, when compared with the control rats. Interestingly, when AgNPs exposure was followed by treatment with RBR, significant reduction of serum urea and creatinine levels was observed when compared with the AgNPs-treated rats.

### Effect of AgNPs and/or RBR juice on electrolytes

In Table 1, it is illustrated that AgNPs treatment induced significant increases of serum potassium and chloride ion levels and a significant decrease in serum calcium ions level in AgNPs-treated rats, when compared with the control animals. However, RBR post-treatment restrained AgNPs toxicity evidenced by significant reductions in potassium and chloride ion levels and significant increase in serum calcium ions level, when compared with AgNPs-only-treated rats. The obtained results showed that the sodium ion levels did not exhibit significant changes between untreated and treated groups.

### Effect of AgNPs and/or RBR juice on kidney oxidative stress

Figure 2 indicated that AgNPs-treated rats exhibited a significant increase in kidney LPO level, and a significant decline in kidney reduced glutathione (GSH) content as well as SOD and CAT activities, when compared with the normal control group. Treatment of AgNPs with RBR (AgNPs + RBR) presented a significantly decreased kidney LPO level and a significant increment in kidney GSH content as well as of catalase and SOD activities, when compared with AgNPs-treated rats.

### Kidney DNA fragmentation in rats treated with AgNPs and/or RBR juice

After undergoing AgNPs treatment, AgNPs-treated rats exhibited a significant increase in kidney DNA damage ( $P < 0.05$ ), indicated by an increment in tail length, tail DNA% and tail movement, when compared with the normal control and RBR rats. In AgNPs + RBR rats, the subsequent treatment of AgNPs exposure with *Beta vulgaris* (AgNPs + RBR) exhibited a significant reduction of this elevated kidney DNA damage, when compared with AgNPs-treated rats (Table 2).

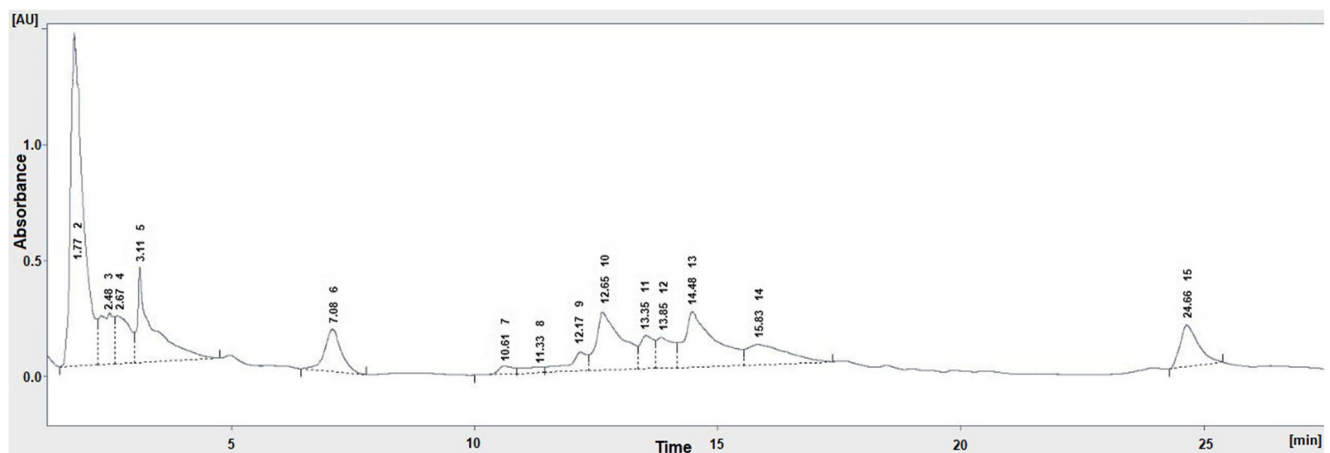


Fig. 1 The HPLC fingerprint (280 nm) of red beetroot juice

**Table 1** Changes in kidney function parameters (urea and creatinine) and serum electrolytes (sodium, potassium, chloride and calcium ions) in different groups

Group	Urea (mg/dL)	Creatinine (mg/dL)	Na <sup>+</sup> (mmol/L)	K <sup>+</sup> (mmol/L)	Ca <sup>++</sup> (mmol/L)	Cl <sup>-</sup> (mmol/L)
Control	34.0 ± 1.05 <sup>#</sup>	0.512 ± 0.04 <sup>#</sup>	135.4 ± 0.32 <sup>#</sup>	4.12 ± 0.09 <sup>#</sup>	1.25 ± 0.02 <sup>#</sup>	101.6 ± 0.58 <sup>#</sup>
RBR	28.6 ± 1.03 <sup>S</sup>	0.474 ± 0.04 <sup>#</sup>	135.5 ± 0.25 <sup>#</sup>	3.98 ± 0.08 <sup>#</sup>	1.25 ± 0.03 <sup>#</sup>	100.7 ± 0.77 <sup>#</sup>
AgNPs	47.2 ± 1.36 <sup>@</sup>	0.678 ± 0.04 <sup>S</sup>	134.2 ± 1.35 <sup>#</sup>	5.51 ± 0.15 <sup>@</sup>	1.02 ± 0.11 <sup>@</sup>	118.0 ± 1.93 <sup>S</sup>
AgNPs + RBR	32.4 ± 1.36 <sup>#</sup>	0.548 ± 0.02 <sup>#</sup>	133.7 ± 0.71 <sup>#</sup>	5.04 ± 0.07 <sup>S</sup>	1.16 ± 0.02 <sup>S</sup>	106.4 ± 0.89 <sup>#</sup>

The values are the samples mean ± SE (n = 10). Columns with different symbols are statistically significant at p < 0.05

### Effect of AgNPs and/or RBR juice on kidney histopathology

Kidney sections in control and RBR-treated rats displayed normal structure of the renal cortex which comprised renal corpuscles and proximal and distal convoluted tubules (Fig. 3 a and b). Kidney sections in chronic AgNPs-treated rats revealed variable pathological changes in glomeruli and some parts of the urinary tubules, identified as loss of characteristic configuration of malpighian corpuscles, mild cell infiltration, necrosis, strong atrophied and vacuolated renal tubules (Fig. 3c). Consistent with the microscopic findings, the semi-quantitative analysis revealed a marked increase in the total score compared with the control group (Supplementary data; Figure S1). Furthermore, the quantitative analysis of the glomerular-capillary tuft area and glomerulus diameter revealed a

significant decrease in rats exposed to AgNPs (Supplementary data; Figure S1). Kidney sections from treated AgNPs + RBR rats showed preserved organisation of tubular and glomerular structures with well-established epithelia resembling that of the control group, except for mild atrophied and/or vacuolated renal tubules (Fig. 3d and Supplementary data; Figure S1). To some extent, the glomerular-capillary tuft area and glomerulus diameter were partially restored in comparison with the AgNPs-treated rats (Supplementary data; Figure S1).

Furthermore, toluidine blue staining revealed the presence of AgNPs precipitates within the cytoplasm of renal cells in group 3 rats, AgNPs-treated (Fig. 4c). However, the number of AgNPs precipitates within the renal cells decreased in kidney section of group 4 rats, post-treated with the RBR (AgNPs + RBR) (Fig. 4d). These data suggest the ability of RBR to facilitate AgNPs removal from the kidney tissue.

**Fig. 2** Renal LPO and GSH levels and SOD and CAT activities following silver nanoparticles (AgNPs, 80 mg/kg; > 100 nm) and/or beetroot juice (RBR, 200 mg/kg, orally) exposure in male rats. The values are the samples mean ± SE (n = 10). Columns with different symbols are statistically significant at p < 0.05

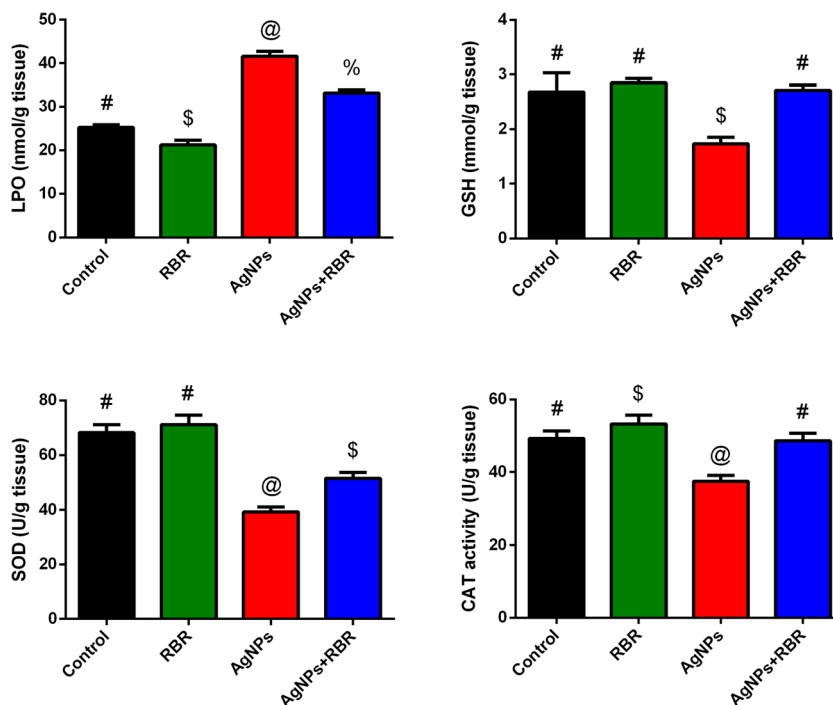


**Table 2** Kidney DNA damage (comet assay parameters obtained by image analysis in cells) in different groups

Group	Tailed %	Untailed %	Tail length $\mu\text{m}$	Tail DNA%	Tail moment
Control	3	97	$1.83 \pm 0.09$	1.70	2.98
RBR	2	98	$1.52 \pm 0.28$	1.46	1.96
AgNPs	13	87	$5.93 \pm 0.22^*$	3.59*	15.81*
AgNPs + RBR	5	95	$2.05 \pm 0.21^{*\#}$	2.31 <sup>#</sup>	4.18 <sup>#</sup>

RBR red beetroot, AgNPs silver nanoparticles, AgNPs + RBR silver nanoparticles with red beetroot group

\*significant difference compared with the control group

<sup>#</sup> significant difference compared with the AgNPs group

### Effect of AgNPs and/or RBR juice on kidney Bcl-2 expressions

Expression of cytoplasmic anti-apoptotic Bcl-2 was strongly detected in kidney sections in control and RBR animals (Fig. 5 a and b). On the other hand, Fig. 5c showed mild Bcl-2 expression in kidney sections of AgNPs-treated rats, while AgNPs + RBR-treated rats' kidney sections revealed moderate positive staining for Bcl-2 expression (Fig. 5d).

### Discussion

In the present study, AgNPs toxicity was analysed on kidneys of adult male rats. Chronic AgNPs treatment induced renal toxicity evidenced by a rise in kidney function markers and by disturbance of serum electrolyte levels. These biochemical alterations were accompanied by DNA damage, oxidative stress and apoptosis events. The obtained results are in accordance with findings of Wen et al. (2017): they found that a

single injection of 5 mg/kg AgNPs, with a 27.3–106.2-nm diameter range, caused genotoxicity and cytotoxicity in the kidney principally but also in the liver to some degree. Growing evidence from previous studies demonstrated that AgNPs translocated and accumulated into kidneys and other specific target tissues, where further processing into free Ag<sup>+</sup> may occur (Park et al. 2011b; Wen et al. 2017). The accepted explanation for toxicity induced by AgNPs lays its ability to release Ag ions, causing inflammatory cell infiltration. These cells play a fundamental role in reactive oxygen species (ROS) generation leading to tissue oxidative injury (Yun et al. 2015).

In in vivo and in vitro studies, the size of Ag nanoparticles is a significant factor. According to Hamouda et al. (2019), the biosynthesis of AgNPs with a diameter less than 30 nm produced a toxic compound, whereas 30–100-nm diameter AgNPs were less toxic because the particles cannot penetrate deeply into tissues and cells. Similarly, particle diameter dependent toxicity was demonstrated by Park et al. (2011a): they illustrated that 5-nm diameter AgNPs were highly toxic for

**Fig. 3** a–d Photomicrographs of rat kidney sections of different experimental groups stained with haematoxylin and eosin. a, b Kidney sections of control and RBR-only-treated groups showing normal structure of glomeruli (G) and urinary tubules (RT). c Kidney sections from chronic AgNPs-treated rat revealing lost characteristic configuration of malpighian corpuscles (G), mild cell infiltration, necrosis, strong atrophied and vacuolated renal tubules (arrows). d Kidney sections from AgNPs + RBR-treated rat showing mild atrophied and/or vacuolated renal tubules (arrows). Scale bar = 25  $\mu\text{m}$

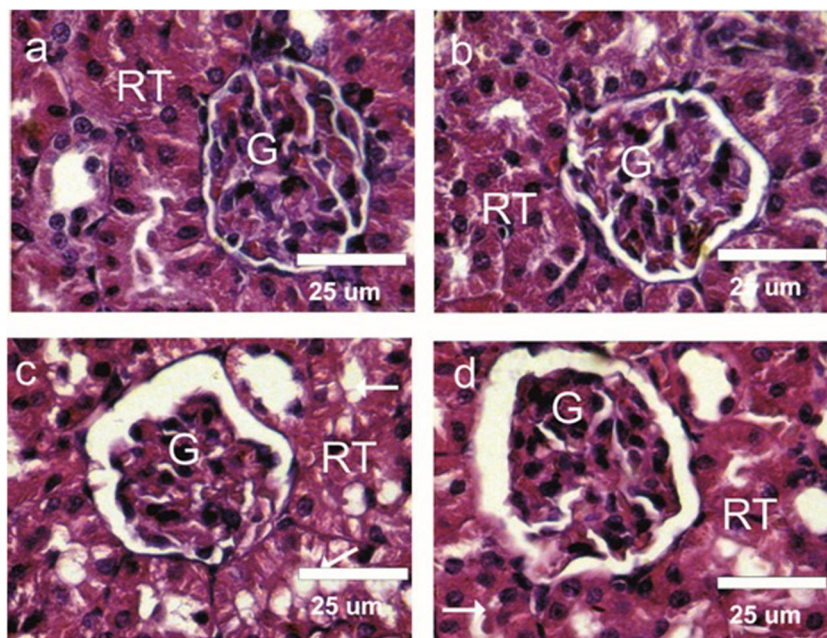
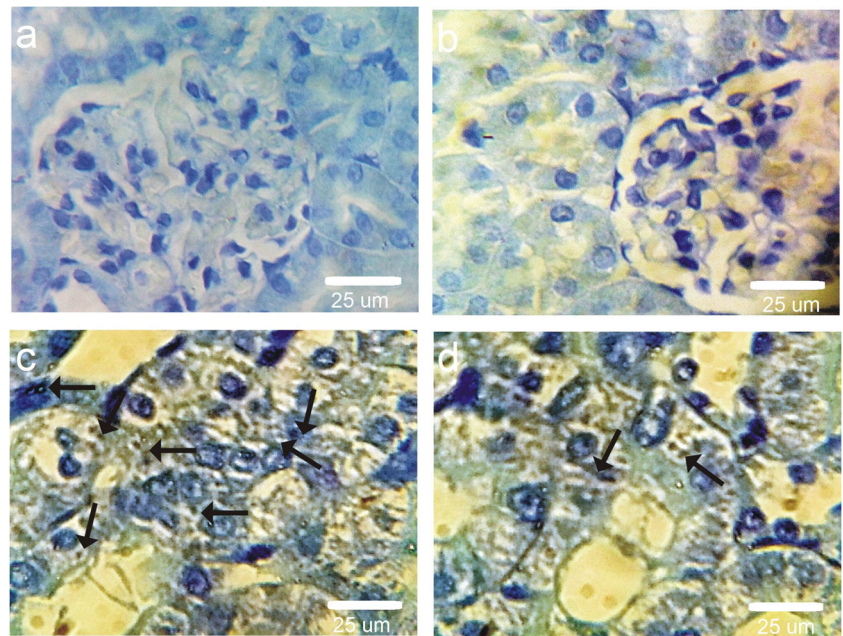


**Fig. 4** Photomicrographs showing AgNPs precipitation in kidney tissues from different groups using toluidine blue method. **a** control, **b** RBR, **c** AgNPs, **d** AgNPs + RBR groups. Arrow reveals the precipitation of AgNPs within the renal cells. Scale bar = 50  $\mu$ m

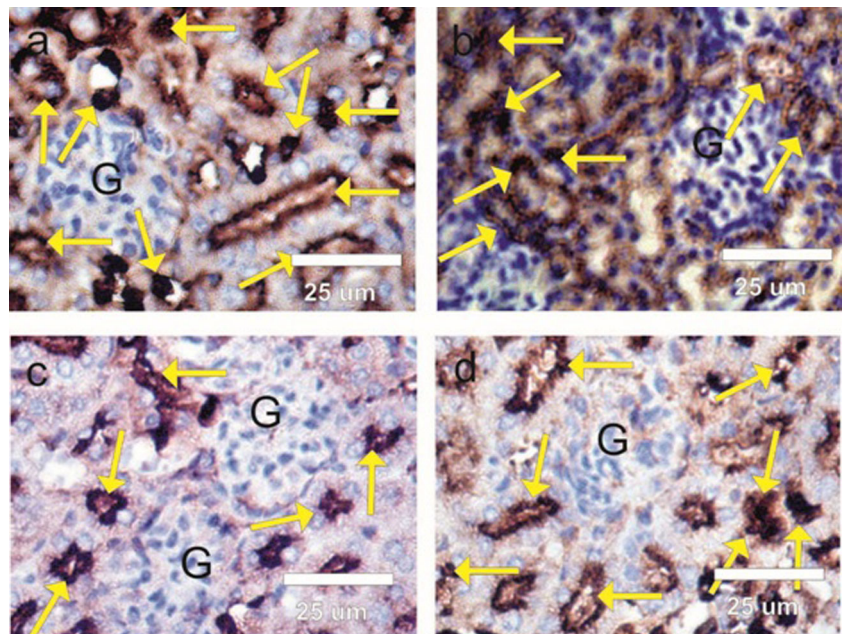


HEI-OC1 and HaCaT cells, followed by 25-, 50- and 110-nm diameter particles. Furthermore, Wang et al. (2014) found that 20-nm diameter polyvinylpyrrolidone and citrate-coated AgNPs induced more cellular toxicity and oxidative stress than larger (110-nm diameter) particles. This was due to a higher rate of dissolution and of Ag<sup>+</sup> bioavailability, which caused acute neutrophilic inflammation in the lungs of intoxicated mice. Therefore, the previous reports indicated that AgNPs diameter may be considered as a major factor determining its toxicity.

In the present study, silver concentration was elevated in kidney tissue upon AgNPs administration for four weeks. Our

findings agree with the previous study by Recordati et al. (2016). These authors demonstrated that AgNPs are able to enter cells by simple diffusion or endocytosis leading to renal dysfunction described by observing increased kidney biomarkers. Moreover, Yang et al. (2017) reported that 10 mg/kg AgNPs at a diameter size of 3 nm accumulated in preference in kidneys, as opposed to other vital organs, causing pathological changes within the tissue. Interestingly, post-administration of RBR effectively reduced Ag levels, suggesting a role for RBR in the ability to promote Ag clearance and excretion. RBR is rich in flavonoids that have hydroxyl and oxo-groups. These interact with Ag ions facilitating their

**Fig. 5 a–d** Photomicrographs of rat kidney sections showing immunohistochemical analysis of anti-apoptotic Bcl-2 in different groups under study. **a**, **b** Strong positive detection (arrows) of Bcl-2 in rat kidney sections of control and RBR-only-treated groups. **c** Mild positive detection (arrows) of Bcl-2 in kidney sections of AgNPs-treated rats. **d** Moderate positive detection (arrows) of Bcl-2 in kidney sections of AgNPs + RBR-treated rats. Scale bar = 25  $\mu$ m



clearance as a chelating agent (Almeer et al. 2018). The chelation capacity of RBR has been previously documented (Wruss et al. 2015). As a result of Ag clearance, RBR prevented the occurrence of pathological changes and restored renal function marker levels to the control values.

In this study, the subchronic administration of AgNPs induced kidney injury, evidenced by increased creatinine, urea and electrolyte levels. Our findings are in agreement with the results achieved by Tiwari et al. (2017): they found that 60-day-long administration of 50 ppm and 200 ppm AgNPs led to renal toxicity in female Wistar rats. In addition, Milić et al. (2015) found that 50 and 100 mg/L AgNPs produced damage to porcine kidney (Pk15) cells; and Vasanth and Kurian (2017) demonstrated that oral administration of AgNPs (100 mg/kg) for 15 days induced kidney injury and dysfunction in rats. Interestingly, RBR post-treatment significantly prevented AgNPs-induced elevations in serum creatinine and urea as well as in disturbance of electrolyte levels. This indicates that RBR carries kidney protection activities probably by safeguarding membrane integrity and kidney function preventing these marker accumulations in the blood. The obtained results agree with a previous study performed by El Gamal et al. (2014): they reported that repeated administration of RBR prevented renal damage in gentamicin-induced toxicity in rats. In addition, our findings are consistent with study results from Albasher et al. (2019): they showed that RBR pre-administration protected kidney tissue against chlorpyrifos-induced renal toxicity. Furthermore, Cheng et al. (2019) recently found that chlorogenic acid that is found in RBR prevented lead-induced nephrotoxicity by its ability to prevent oxidative stress-induced disturbance in kidney markers.

In the present study performed in adult male rats, AgNPs intoxication elevated significantly LPO level and depleted substantially the reduced GSH content in the kidney. In addition, it inhibited SOD and CAT activities. Our findings indicated that AgNPs may induce oxidative stress through a ROS-mediated process. AgNPs nephrotoxicity appears to increase ROS generation through discharge of  $\text{Ag}^+$  ions within the cells compartments. In fact, Lee et al. (2019) documented that exposure to AgNPs (100 nm) increased hydroxyl radical generation, causing a mitochondrial membrane potential drop and cell death in fungi. Furthermore, Radhakrishnan et al. (2018) reported that both ROS-dependent and ROS-independent pathways appear to be involved in triggering cell death in *Candida albicans* when treated with 10–30 nm AgNPs. Additionally, Barcinska et al. (2018) found that the anticancer activity of AgNPs has been due to its increased ability to induce oxidative and nitrosative stresses. In addition, the same authors found that AgNPs (2.6 and 18 nm) suppressed the antioxidant defence system and potentially down-regulated gene expression of antioxidant enzymes in pancreatic ductal adenocarcinoma cells (PANC-1). Remarkably, all these disruptions can be prevented by post-administration with RBR. The antioxidant effect of RBR was demonstrated by the

significant reduction in LPO and increment in the enzymatic and non-enzymatic antioxidant protein production in kidney tissues. Several studies reported the free radical quenching properties of RBR (Amaral et al. 2019; Lorizola et al. 2018). RBR is an outstandingly rich source of antioxidant ingredients such as betalain, rutin, epicatechin and caffeic acid (Clifford et al. 2015). The antiradical activity of these ingredients is attributed to their electron-donating capacity promoting the defusing of highly reactive radicals targeting cellular membranes. In particular, the NO donation of RBR has been shown to inhibit free radical generation and to directly scavenge potentially damaging ROS (Albasher et al. 2019). Moreover, RBR demonstrated indirect antioxidant effects by acting as stimulator of gene expression of the antioxidant defence system (Vulić et al. 2014). The present results are in accordance with the previous studies; these demonstrated the capability of RBR active ingredients such as protocatechuic and ferulic acids to mitigate heavy metal-induced nephrotoxicity by enhancing the antioxidant defence mechanism (Adefegha et al. 2016; Al Olayan et al. 2020). Likewise, in the current study, RBR post-administration restored the endogenous antioxidant defence system to normal cellular concentrations following AgNPs exposure.

Following AgNPs intoxication, oxidative stress and excessive generation of ROS in renal cells led to apoptosis. Our findings are in accordance with previous results reported by Mytych et al. (2017): they found that AgNPs caused DNA adducts, DNA breaks, oxidative DNA injury and micronuclei formation and that it may encourage genotoxicity. Furthermore, AgNPs-mediated apoptotic cell death and/or neurodegeneration were promoted via calcium dysregulation in neuronal cells. AgNPs-induced apoptosis involved a mitochondrial pathway: AgNPs treatment resulted in cytochrome *c* discharge into the cytoplasm and in Bax translocation from cytoplasm to mitochondria in NIH3T3 fibroblast cells and human Chang liver cells (Piao et al., 2011). The present results are in agreement with other studies, such as a new one by Gurunathan et al. (2018) who found that AgNPs induce cell death in A549 lung cells through a mitochondrial-mediated intrinsic apoptotic pathway. Bcl-2 was localised in the mitochondria outer membrane and played a central role in promoting cellular survival and in inhibiting the actions of pro-apoptotic proteins (AL-Megrin et al. 2020). RBR post-treatment promoted Bcl-2 expression in kidney tissues. Recently, Albasher et al. (2019) found that RBR treatment enhanced anti-apoptotic proteins and restrained pro-apoptotic proteins in response to toxicant. Thus, our data indicated that RBR protects against AgNPs-induced nephrotoxicity in rats by modulating the apoptotic pathway.

In conclusion, the present study indicates that RBR has a renal protective potential. The nephroprotective effect of RBR against AgNPs-induced nephrotoxicity may be ascribed to its antioxidant and anti-apoptosis properties. Our results substantiate the use of RBR in folk medicine for the treatment of renal diseases.



**Funding information** This research was funded by the Deanship of Scientific Research at Princess Nourah bint Abdulrahman University through the Fast-track Research Funding Program.

## Compliance with ethical standards

The study protocols were approved by the Ethics Committee for Laboratory Animal Care of Princess Nourah bint Abdulrahman University in Riyadh (KSA; H-01-R-059; IRB long number: 19-0201).

## References

- Abd El-Ghffar EA et al (2019) HPLC-ESI- MS/MS analysis of beet (*Beta vulgaris*) leaves and its beneficial properties in type 1 diabetic rats. *Biomedicine & Pharmacotherapy* 120:109541. <https://doi.org/10.1016/j.biopha.2019.109541>
- Abdel Moneim AE (2013) The neuroprotective effects of purslane (*Portulaca oleracea*) on rotenone-induced biochemical changes and apoptosis in brain of rat CNS. *Neurol Disord Drug Targets*
- Abramenko NB, Demidova TB, Abkhalimov EV, Ershov BG, Krysanov EY, Kustov LM (2018) Ecotoxicity of different-shaped silver nanoparticles: case of zebrafish embryos. *J Hazard Mater* 347:89–94
- Adefegha SA, Omojokun OS, Oboh G, Fasakin O, Ogunsuyi O (2016) Modulatory effects of ferulic acid on cadmium-induced brain damage. *J Evid Based Complementary Altern Med* 21:NP56–NP61
- Aebi H (1984) Catalase in vitro. *Methods Enzymol* 105:121–126
- Al Olayan EM, Aloufi AS, AlAmri OD, El-Habit OH, Abdel Moneim AE (2020) Protocatechuic acid mitigates cadmium-induced neurotoxicity in rats: role of oxidative stress, inflammation and apoptosis. *Sci Total Environ* 723:137969 <https://doi.org/10.1016/j.scitotenv.2020.137969>
- Alajmi RA et al. (2019) Anti-toxoplasma activity of silver nanoparticles green synthesized with Phoenix dactylifera and Ziziphus spinachristi extracts which inhibits inflammation through liver regulation of cytokines in Balb/c mice *Biosci Rep* 39 doi:BSR20190379
- Albasher G, Albrahim T, Alsultan N, Alfaraj S, Alharthi MS, Kassab RB, Abdel Moneim AE (2019) Red beetroot extract mitigates chlorpyrifos-induced reprotoxicity associated with oxidative stress, inflammation, and apoptosis in rats *Environmental science and pollution research international* doi:<https://doi.org/10.1007/s11356-019-07009-6>
- Almeer RS et al. (2018) Royal jelly abrogates cadmium-induced oxidative challenge in mouse testes: involvement of the Nrf2 pathway *International journal of molecular sciences* 19 doi:<https://doi.org/10.3390/ijms19123979>
- AL-Megrin WA, Soliman D, Kassab RB, Metwally DM, Ahmed E, Abdel Moneim, El-Khadragy MF (2020) Coenzyme q10 activates the antioxidant machinery and inhibits the inflammatory and apoptotic cascades against lead acetate-induced renal injury in rats. *Frontiers in Physiology* 11 <https://doi.org/10.3389/fphys.2020.00064>
- Amaral AL et al. (2019) A single dose of beetroot juice does not change blood pressure response mediated by acute aerobic exercise in hypertensive postmenopausal women *Nutrients* 11 doi:nu11061327
- Bao S, Tang W, Fang T (2020) Sex-dependent and organ-specific toxicity of silver nanoparticles in livers and intestines of adult zebrafish *Chemosphere* 249:126172
- Barcinska E, Wierzbička J, Zauszkiewicz-Pawlak A, Jacewicz D, Dabrowska A, Inkielewicz-Stepniak I (2018) Role of oxidative and nitro-oxidative damage in silver nanoparticles cytotoxic effect against human pancreatic ductal adenocarcinoma cells *Oxid Med Cell Longev* 2018:8251961 doi:<https://doi.org/10.1155/2018/8251961>
- Cheng D, Li H, Zhou J, Wang S (2019) Chlorogenic acid relieves lead-induced cognitive impairments and hepato-renal damage via regulating the dysbiosis of the gut microbiota in mice. *Food & function* 10:681–690 doi:<https://doi.org/10.1039/c8fo01755g>
- Clifford T, Howatson G, West DJ, Stevenson EJ (2015) The potential benefits of red beetroot supplementation in health and disease. *Nutrients* 7:2801–2822
- Daoust R, Molnar F (1964) Cellular populations and mitotic activity in rat liver parenchyma during azo dye carcinogenesis. *Cancer Res* 24:1898–1909
- Drury RAD, Wallington EA (1981) *Carleton's Histological Technique* Oxford University Press, New York
- El Gamal AA et al. (2014) Beetroot (*Beta vulgaris* L.) extract ameliorates gentamicin-induced nephrotoxicity associated oxidative stress, inflammation, and apoptosis in rodent Model *Mediators of Inflammation* 2014:12 doi:<https://doi.org/10.1155/2014/983952>
- El-Borady OM, Othman MS, Atallah HH, Abdel Moneim AE (2020) Hypoglycemic potential of selenium nanoparticles capped with polyvinyl-pyrrolidone in streptozotocin-induced experimental diabetes in rats. *Heliyon* 6 <https://doi.org/10.1016/j.heliyon.2020.e04045>
- El-Khadragy M et al. (2018) Clinical efficacy associated with enhanced antioxidant enzyme activities of silver nanoparticles biosynthesized using *Moringa oleifera* Leaf extract, against cutaneous leishmaniasis in a murine model of *Leishmania major* *Int J Environ Res Public Health* 15 doi:ijerph15051037
- Ellman GL (1959) Tissue sulfhydryl groups. *Arch Biochem Biophys* 82:70–77
- Fukushima T, Jintana W, Okabe S (2020) Mixture toxicity of the combinations of silver nanoparticles and environmental pollutants *Environmental science and pollution research international* 27:6326–6337 doi:<https://doi.org/10.1007/s11356-019-07413-y>
- Gurunathan S, Kang MH, Kim JH (2018) Combination effect of silver nanoparticles and histone deacetylases inhibitor in human alveolar basal epithelial cells *Molecules* 23
- Hamouda RA, Hussein MH, Abo-elmagd RA, Bawazir SS (2019) Synthesis and biological characterization of silver nanoparticles derived from the cyanobacterium *Oscillatoria limnetica* *Scientific Reports* 9:13071 doi:<https://doi.org/10.1038/s41598-019-49444-y>
- Harrison-Bernard LM, Navar LG, Ho MM, Vinson GP, El-Dahr SS (1997) Immunohistochemical localization of ANG II AT1 receptor in adult rat kidney using a monoclonal antibody *Am J Physiol* 273:F170–F177 <https://doi.org/10.1152/ajprenal.1997.273.1.F170>
- Jain NK, Singhai AK (2012) Protective role of *Beta vulgaris* L. leaves extract and fractions on ethanol-mediated hepatic toxicity. *Acta Pol Pharm* 69:945–950
- Kim YS et al. (2010) Subchronic oral toxicity of silver nanoparticles. *Part Fibre Toxicol* 7:20
- Lee B, Lee MJ, Yun SJ, Kim K, Choi IH, Park S (2019) Silver nanoparticles induce reactive oxygen species-mediated cell cycle delay and synergistic cytotoxicity with 3-bromopyruvate in *Candida albicans*, but not in *Saccharomyces cerevisiae*. *Int J Nanomedicine* 14:4801–4816 <https://doi.org/10.2147/IJN.S205736>
- Lekame S, Miranda AF, Abraham A, Li V, Shukla R, Bansal V, Nugegoda D (2018) The toxicity of silver nanoparticles (AgNPs) to three freshwater invertebrates with different life strategies: *Hydra vulgaris*, *Daphnia carinata*, and *Paratya australiensis* *Frontiers in Environmental Science* 6 doi:<https://doi.org/10.3389/fenvs.2018.00152>
- Li L et al. (2018) Silver nanoparticles induce SH-SY5Y cell apoptosis via endoplasmic reticulum- and mitochondrial pathways that lengthen endoplasmic reticulum-mitochondria contact sites and alter inositol-3-phosphate receptor function *Toxicol Lett* 285:156–167
- Lorizola IM et al. (2018) Beet stalks and leaves (*Beta vulgaris* L.) protect against high-fat diet-induced oxidative damage in the liver in mice *Nutrients* 10

- Martinez RM et al. (2015) Anti-inflammatory activity of betalain-rich dye of Beta vulgaris: effect on edema, leukocyte recruitment, superoxide anion and cytokine production Arch Pharm Res 38:494-504 <https://doi.org/10.1007/s12272-014-0473-7>
- Milić M, Leitinger G, Pavičić I, Zebić Avdičević M, Dobrović S, Goessler W, Vinković Vrček I (2015) Cellular uptake and toxicity effects of silver nanoparticles in mammalian kidney cells Journal of Applied Toxicology 35:581-592 doi:<https://doi.org/10.1002/jat.3081>
- Mohammed HS, Abdel-Aziz MM, Abu-Baker MS, Saad AM, Mohamed MA, Ghareeb MA (2019) Antibacterial and potential antidiabetic activities of flavone c-glycosides isolated from Beta vulgaris subspecies cicla L. var. Flavescens (Amaranthaceae) cultivated in Egypt Curr Pharm Biotechnol 20:595-604 doi:CPB-EPUB-98793
- Mytych J, Zebrowski J, Lewinska A, Wnuk M (2017) Prolonged effects of silver nanoparticles on p53/p21 pathway-mediated proliferation, DNA damage response, and methylation parameters in ht22 hippocampal neuronal cells Mol Neurobiol 54:1285-1300. <https://doi.org/10.1007/s12035-016-9688-6>
- Nishikimi M, Appaji N, Yagi K (1972) The occurrence of superoxide anion in the reaction of reduced phenazine methosulfate and molecular oxygen Biochem Biophys Res Commun 46:849-854
- Ohkawa H, Ohishi N, Yagi K (1979) Assay for lipid peroxides in animal tissues by thiobarbituric acid reaction Anal Biochem 95:351-358
- Olive PL, Banáth JP (2006) The comet assay: a method to measure DNA damage in individual cells Nature Protocols 1:23-29 doi:<https://doi.org/10.1038/nprot.2006.5>
- Park J et al. (2011a) Size dependent macrophage responses and toxicological effects of Ag nanoparticles Chem Commun (Camb) 47:4382-4384 doi:<https://doi.org/10.1039/c1cc10357a>
- Park K, Park EJ, Chun IK, Choi K, Lee SH, Yoon J, Lee BC (2011b) Bioavailability and toxicokinetics of citrate-coated silver nanoparticles in rats. Arch Pharm Res 34:153-158 doi:<https://doi.org/10.1007/s12272-011-0118-z>
- Racusen LC et al. (1999) The Banff 97 working classification of renal allograft pathology. Kidney Int 55:713-723 doi:<https://doi.org/10.1046/j.1523-1755.1999.00299.x>
- Radhakrishnan VS, Dwivedi SP, Siddiqui MH, Prasad T (2018) In vitro studies on oxidative stress-independent, Ag nanoparticles-induced cell toxicity of Candida albicans, an opportunistic pathogen Int J Nanomedicine 13:91-96 doi:<https://doi.org/10.2147/IJN.S125010>
- Recordati C et al. (2016) Tissue distribution and acute toxicity of silver after single intravenous administration in mice: nano-specific and size-dependent effects Part Fibre Toxicol 13:12 doi:<https://doi.org/10.1186/s12989-016-0124-x>
- Singh A, Dar MY, Joshi B, Sharma B, Shrivastava S, Shukla S (2018) Phytofabrication of silver nanoparticles: novel drug to overcome hepatocellular ailments. Toxicology Reports 5:333-342 doi:<https://doi.org/10.1016/j.toxrep.2018.02.013>
- Szaefer H, Krajka-Kuzniak V, Ignatowicz E, Adamska T, Baer-Dubowska W (2014) Evaluation of the effect of beetroot juice on DMBA-induced damage in liver and mammary gland of female Sprague-Dawley rats Phytotherapy research : PTR 28:55-61 doi: <https://doi.org/10.1002/ptr.4951>
- Tiwari R et al. (2017) Oral subchronic exposure to silver nanoparticles causes renal damage through apoptotic impairment and necrotic cell death. Nanotoxicology 11:671-686 doi:<https://doi.org/10.1080/17435390.2017.1343874>
- Tortella GR, Rubilar O, Duran N, Diez MC, Martinez M, Parada J, Seabra AB (2020) Silver nanoparticles: toxicity in model organisms as an overview of its hazard for human health and the environment J Hazard Mater 390:121974 doi:S0304-3894(19)31928-4
- Vasanth SB, Kurian GA (2017) Toxicity evaluation of silver nanoparticles synthesized by chemical and green route in different experimental models Artificial Cells, Nanomedicine, and Biotechnology 45:1721-1727 doi:<https://doi.org/10.1080/21691401.2017.1282500>
- Vulić JJ, Čebović TN, Čanadanović-Brunet JM, Četković GS, Čanadanović VM, Djilas SM, Tumbas Šaponjac VT (2014) In vivo and in vitro antioxidant effects of beetroot pomace extracts. Journal of Functional Foods 6:168-175 doi:<https://doi.org/10.1016/j.jff.2013.10.003>
- Wang X et al. (2014) Use of coated silver nanoparticles to understand the relationship of particle dissolution and bioavailability to cell and lung toxicological potential Small 10:385-398 doi:<https://doi.org/10.1002/smll.201301597>
- Wen H et al. (2017) Acute toxicity and genotoxicity of silver nanoparticle in rats PLoS One 12:e0185554 doi:<https://doi.org/10.1371/journal.pone.0185554>
- Wruss J et al. (2015) Compositional characteristics of commercial beetroot products and beetroot juice prepared from seven beetroot varieties grown in Upper Austria. Journal of Food Composition and Analysis 42:46-55 doi:<https://doi.org/10.1016/j.jfca.2015.03.005>
- Yang L, Kuang H, Zhang W, Aguilar ZP, Wei H, Xu H (2017) Comparisons of the biodistribution and toxicological examinations after repeated intravenous administration of silver and gold nanoparticles in mice Sci Rep 7:3303 doi:<https://doi.org/10.1038/s41598-017-03015-1>
- Yun JW et al (2015) Comparative toxicity of silicon dioxide, silver and iron oxide nanoparticles after repeated oral administration to rats. J Appl Toxicol 35:681–693. <https://doi.org/10.1002/jat.3125>

**Publisher's note** Springer Nature remains neutral with regard to jurisdictional claims in published maps and institutional affiliations.